

# NATURAL CONVECTION AND HEAT TRANSFER IN THE PCB'S ARRAY OF ELECTRONIC EQUIPMENTS

Zhiguo Wang, F. Mayinger

Lehrstuhl A für Thermodynamik, TU München, 8000 Munich 2, F.R.G.

## ABSTRACT

This paper presents the results of an experimental study of natural convective air cooling in one type of electronic equipments which contain several printed circuit boards (PCB's) set up vertically and parallel to one another in an impervious casing. The behaviour of natural convective air cooling in this kind of PCB's array has been investigated with the aid of holographic interferometry. The results show that the heat transfer in the PCB's array is greatly influenced by an unstable boundary layer and vortex flow near the upper wall of the casing. This influence has, on the one hand, good effects on the cooling of the PCB's, and on the other hand, it brings about unfavourable fluctuations of temperature or heat transfer coefficients on the PCB's. The empirical correlations deduced from the experiments are presented in the form of  $Nu=f(Ra)$  with Rayleigh-number ranging from  $10^2$  to  $10^5$  at  $Pr=0.73$ .

## Introduction

As microelectronic chips continue to decrease in size and to increase in speed and the scale of integrated circuit, the power density, i.e. heat flux of a chip has to be raised to a higher and higher level. Consequently, cooling problems become more and more important in the design of electronic equipments. Because most silicon chips are sensitive to temperature, an adverse thermal environment can cause a malfunction or a fault in an electronic component, which may lead to a system collapse. Since for about every  $20^\circ C$  decrease in the chip temperature the failure rate is reduced by half, a good thermal design is of great importance for electronic equipments.

Natural convection is a cooling technique widely used in electronic equipments with low and medium power density ( $10^2 \sim 10^4 \text{ W/m}^2$ ). It has many advantages such as inherent reliability, low noise and low cost (no fans and blowers are required) etc. Especially in some adverse circumstances where casing must be closed for dust- and water-proof, priority is often given to natural convection cooling scheme. On the other hand, however, natural convection has lower ability of removal of heat than other cooling technique such as forced convection. Therefore, in the thermal design of electronic equipments with natural convection as the thermal control technique, it is necessary to investigate in detail the processes of fluid flow and heat transfer in order to achieve the optimum cooling effect.

Although much work has been done on various natural convective air cooling at chip level, module level, and PCB's level of electronic equipments [1], few results are available at the system level. In ref.[2,3] a correlation of natural convection heat transfer between two parallel plates was presented and the influence of the plate spacing on heat transfer was discussed. A empirical formula based on the experimental results for thermal design of natural-air-cooled electronic equipment casings was recommended in ref.[4]. Some factors that influence the natural convection heat transfer in electronic equipments, such as PCB spacing, additional plates, the shape and size of the vents etc., were studied in ref.[5,6,7]. Ref.[8,9] analysed the heat transfer in electronic equipments with the analytical and numerical methods. Due to the limitation of experimental methods and the memory capacity and the speed of computers, it is difficult now to obtain a complete knowledge of the process and the physical mechanism of heat transfer in electronic equipments.

In this paper experimental results of natural convective air cooling in one type of electronic equipments which contains a PCB's array are presented. The natural convection in such PCB's array has been investigated with the holographic interferometry to obtain detail information not only on the local heat transfer coefficient but also on the temperature field in the natural convection flow.

### Problem under Consideration

This work is concerned with obtaining detail information on natural convection and heat transfer in a casing with a PCB's array set up vertically and parallel to one another in an impervious casing. The heat generated by the chips mounted on PCB's is transferred to the surrounding air by conduction, consequently, reaches the walls of the casing by natural convection. In practice two kinds of structures for PCB's array are widely used. The one that PCB's are nakedly set up in the casing, and the another that each PCB is set up together with a magnetic and electrostatic shield against magnetic and electrostatic field in the casing. Because of the use of metal for electrical conduction pathways, uniform heating

accurately characterizes the boundary condition of a PCB densely populated with chips. In this paper, uniform wall temperature (UWT) conditions will be adopted to simulate the PCB's. The investigation under the uniform wall heat flux (UHF) conditions is underway.

### Experimental Apparatus

The experimental apparatus and supplementary instruments used in the experiments are illustrated in Fig.1.

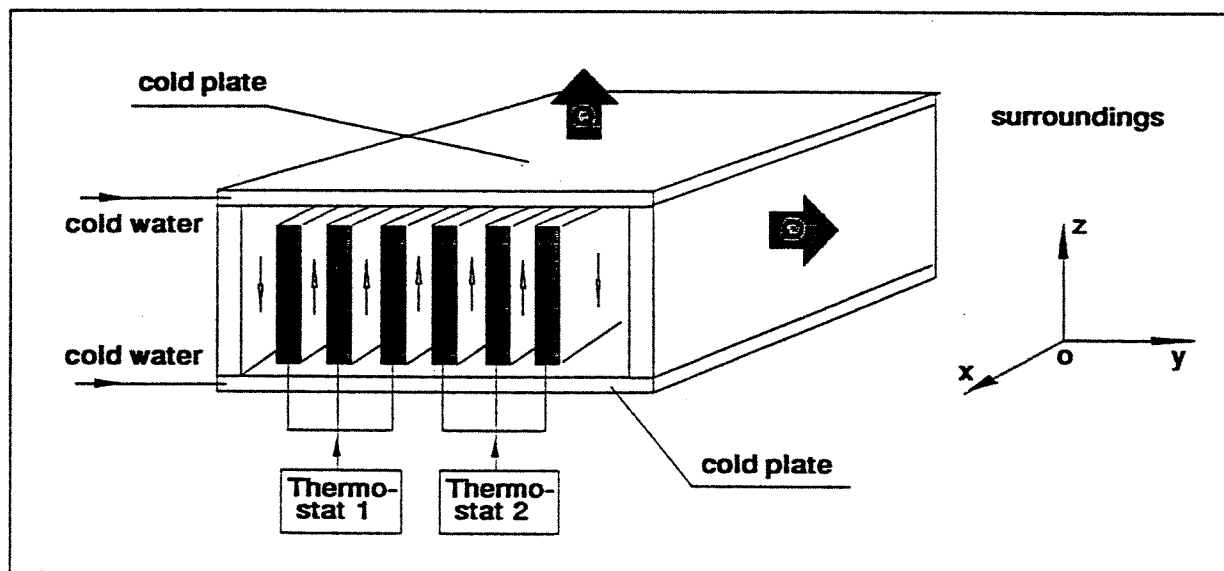


Fig. 1 Schematic drawing of the experimental equipment

The casing simulating the electronic equipment casing was made of aluminium plates. The top and bottom walls were cooled with cold water. The inner aluminium plates simulating PCB's were 10 mm thick and were heated by hot water through S-form slots inside them. Two thermostats were used to heat the water through the inner plates. The temperature of the walls, inner plates, entrances and exits of the thermostats were measured with thermocouples. The spacings between inner plates were equal and could be changed through the number of inner plates and the distance between the inner plates and the top and bottom walls were also adjustable.

### Measuring Technique

Temperature field was measured by means of holographic interferometry. The holographic interferometry, as a measuring technique, has many advantages such as high sensitivity, good accuracy; it does not disturb the flow and temperature field and is an inertialess method. In order to trace the unstable thermal boundary layer occurring in the casing, real

time holographic interferometry was used to visualize the temperature field. The principle of the real time holographic interferometry was discussed in detail in ref. [10]. The optical arrangement of the holographic interferometer is shown in Fig.2.

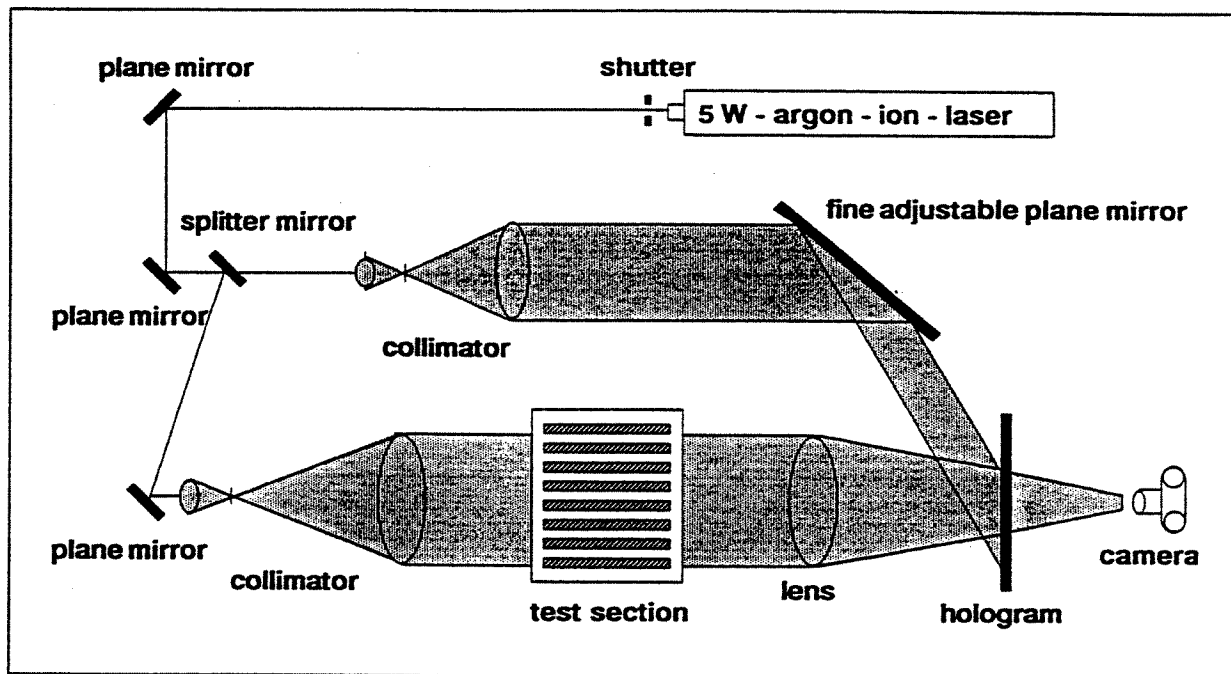


Fig. 2 Optical arrangement of the holographic interferometer

A 5W-argon-ion-laser (Model 2020,  $\lambda = 514.5nm$ ) was used as the light source. By using a beam splitter the light beam from the laser was divided into two parts, i.e., the object beam and the reference beam. Both beams were collimated and expanded into parallel beams. The object beam of 150 mm in diameter passed through the test section and interfered with the reference beam behind the test section on the holographic photoplate. The first exposure was taken under the unheated condition. After processing the photoplate (which is often called hologram) was replaced and illuminated by the same reference beam and then the original object beam could be reconstructed. The optical path length of the object beam passing through the heated test section changed with the variation of the refractive index. The actual object beam interfered with the reconstructed original object beam behind the hologram to make the temperature field visible.

The interference pattern recorded on the film contains information about the temperature field in the test section. For example, the infinite interference fringes indicate the distribution of the isotherms. According to the measured wall temperature and the interference order, the temperature field can be calculated. In an ideal interferometer the optical path length difference between two beams is not dependent on the focusing plane used in making photos because the influence of the light refraction is neglected. But in

non-ideal situations the focusing plane plays an important role in calculating the difference of optical path length. For the problem considered in this paper the temperature gradient was such great that the fringe density could be 9 lines/mm. Hence, the influence of the refraction of light and the focusing plane must be taken into account. According to refs. [11] and [12], if the focusing plane is placed in the test section  $L_z/3$  ( $L_z$  is the length of the test section) apart from the exit, the real difference of optical path length can be calculated by the use of the equation of an ideal interferometry i.e.

$$S \cdot \lambda = \int_0^{L_z} (n_\infty - n) dx = L_z(n_\infty - n) \quad (1)$$

where  $S$  is the interference order,  $\lambda$  the wave length of laser beam,  $L_z$  the length of test section and  $n$  the refractive index of air.

In this experiment the Interference order  $S$  was derived from the measured wall temperature and the recurrence relation of the interference order, and then according to the Gladstone-Dale equation the temperature field was determined from the refractive index with the aid of the state equation of air. Based on the measured temperature field the local heat transfer coefficients were calculated by the use of a polynomial representing the temperature profile. The local Nusselt-number can be expressed as following:

$$Nu = \frac{hb}{k} = \frac{b}{(T_p - T_w)} \frac{\partial T}{\partial n} = f(Ra, r) \quad (2)$$

where  $Nu$  is the local Nusselt-number,  $h$  the heat transfer coefficient,  $b$  the PCB's spacing,  $k$  the thermal conductivity,  $T_p$  the temperature of inner plates,  $T_w$  the temperature of the cold wall,  $Ra$  the channel Rayleigh-number and  $r$  the geometric parameter. The channel Rayleigh-number is defined as:

$$Ra = \frac{g\beta(T_p - T_w)b^4}{\alpha\nu H_p} = Gr_n * Pr * \frac{b}{H_p} \quad (3)$$

We used here the channel Rayleigh-number as a characteristic number because it combines the normal Grashof-number, Prandtl-number and channel  $b/H_p$  ( $H_p$  is height of plate) ratio in one dimensionless group and reduces the number of independent parameters. In addition, it can be also verified with the aid of the dimensional analysis that the behaviour of heat transfer in PCB's array without a casing can be described accurately by using the relation between Nusselt-number and the channel Rayleigh-number, i.e.  $Nu=f(Ra,Pr)$  instead of  $Nu=f(Gr,Pr,b/H_p)$ . The mean Nusselt-number on one PCB is :

$$\overline{Nu} = \frac{1}{H_p} \int_0^{H_p} Nu dz \quad (4)$$

## Results

### 1. Temperature field

Photos of the temperature field in the casing with a PCB's array were taken by means of the holographic interferometry. With an 150mm-in diameter interferometer the temperature variation in the whole casing can be clearly seen. Fig.3 shows the temperature fields in the 3-PCB's, 4-PCB's, 6-PCB's and 8-PCB's arrays respectively.

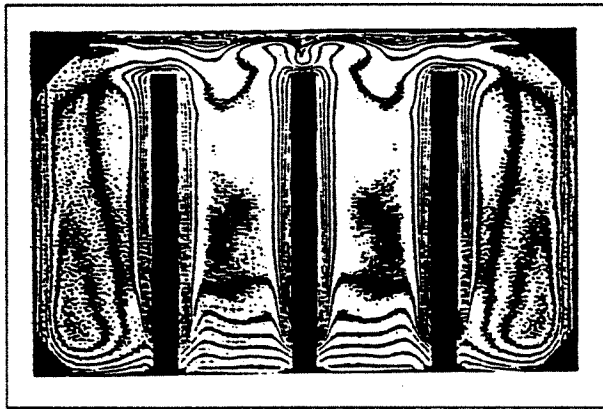


Fig. 3-1 Hologram in a 3-PCB's array  
 $Ra=1.32 \cdot 10^5$ ,  $b=42.5$  mm,  
 $T_w=10^\circ\text{C}$ ,  $T_p=70^\circ\text{C}$ .

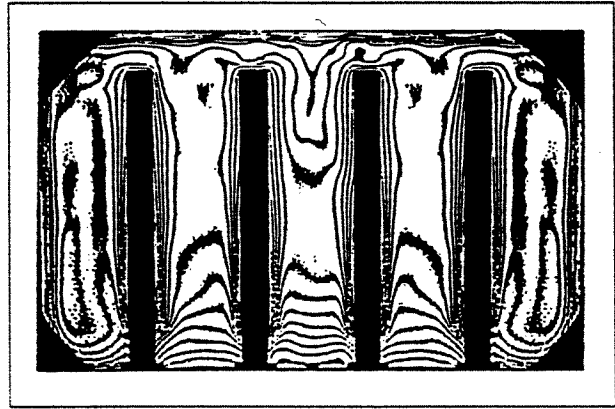


Fig. 3-2 Hologram in a 4-PCB's array  
 $Ra=4.24 \cdot 10^4$ ,  $b=32.0$  mm,  
 $T_w=10^\circ\text{C}$ ,  $T_p=70^\circ\text{C}$ .

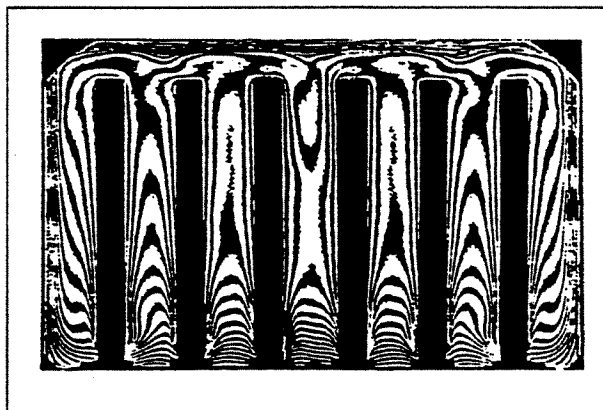


Fig. 3-3 Hologram in a 6-PCB's array  
 $Ra=6.48 \cdot 10^3$ ,  $b=20.0$  mm,  
 $T_w=10^\circ\text{C}$ ,  $T_p=70^\circ\text{C}$ .

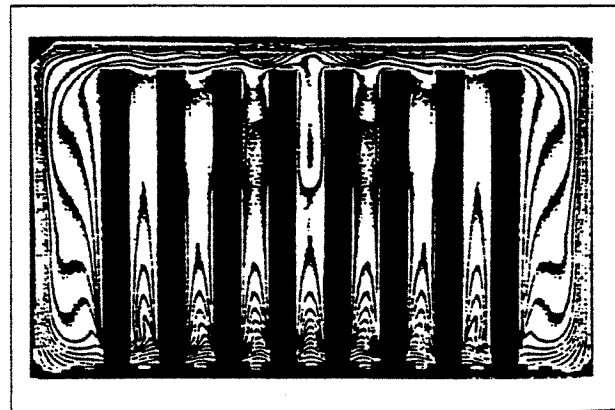


Fig. 3-4 Hologram in a 8-PCB's array  
 $Ra=4.04 \cdot 10^2$ ,  $b=10.0$  mm,  
 $T_w=10^\circ\text{C}$ ,  $T_p=70^\circ\text{C}$ .

Fig. 3 Interferograms in the casing with PCB's arrays

From Fig.3 it can be observed that the thermal boundary layer is presented on the surfaces of inner plates because of the natural convection. When the PCB's spacing is relatively large (e.g. in Fig. 3-1, 3-2 and 3-3), individual thermal boundary layers are in evidence along each surface. In the lower half part of PCB's channels, the thermal boundary layers develop from bottem to top and become thicker and thicker as expected. However in the exit region of the channels, the development of the thermal boundary layer is hindered by the vortex flow which is produced by the thermal instability in the reverse temperature layer on the upper wall. The thickness of the thermal boundary layer is reduced by cold air periodically falling down from upper wall and therefore the thermal boundary layer in the channels has a bulging form. When the PCB's spacing is small enough (e.g. in Fig. 3-4) the developing boundary layers in the channels join together behind a short developing region to form a developed region. On the one hand, it is evident that heat transfer on each PCB is worse than one in the case of large PCB's spacing; On the other hand, the power load on each PCB will be reduced because of available more PCB's at smaller PCB's spacing in the casing. Therefore these effects must be simultaneously considered by the designer of a cooling system of electronic equipments.

On the surface of the upper wall of the casing the thermal boundary layer has the corrugated form as a consequence of the thermally unstable stratification of air in gravitational field and the vortex flow. The temperature profile in the lower part of the plates array is stable because the heated air is above the cooled one. Due to the chimney effect of the channel a entrence region with great temperature variation is produced in this part. Besides, it can also be seen that the thermal boundary layer on the plate surface toward coming flow is much thinner than that on the plate surface back to coming flow.

The periodical change of the thermal unstable boundary layer on the top wall can be recognized in Fig. 4. The cold air on the top wall rips off from the boundray layer and falls down into the PCB's channels, which forms the tongue-form interference pattern in the holograms. The period, penetration and wavelength of this unsteady flow depend on Rayleigh-number, spacings between PCB's and distance between PCB's and top wall. For this example, the period was about 1.5 second and penetration was about 1/3 PCB's height. From Fig.4 it can be seen that the thermal instability has a good effect on the cooling of inner PCB's because it drives the cold air to fall into PCB's array, but it brings about also the unfavourable fluctuations of heat transfer coefficients on the PCB. In the case of UHF it means directly temperature fluctuations on the PCB's.

The temperature and the heat transfer coeffiecient were calculated with the method described in previous section. As an example, temperature profile and the local Nusselt-number at the various points in the 4-PCB's array is shown in Fig.5 and Fig.6 respectively.

Fig. 7 illustrates the local Nusselt-number on the top wall of the casing. The fluctu-

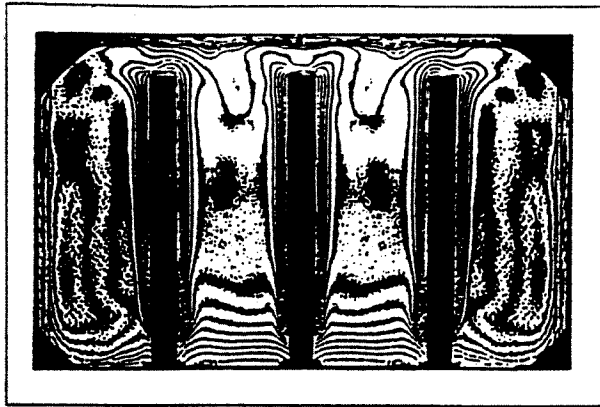


Fig. 4-1 Hologram in a 3-PCB's array  
 $Ra=1.55 \cdot 10^5$ ,  $t=t_0+0.0$  s,  
 $T_w=10^\circ\text{C}$ ,  $T_p=90^\circ\text{C}$ .

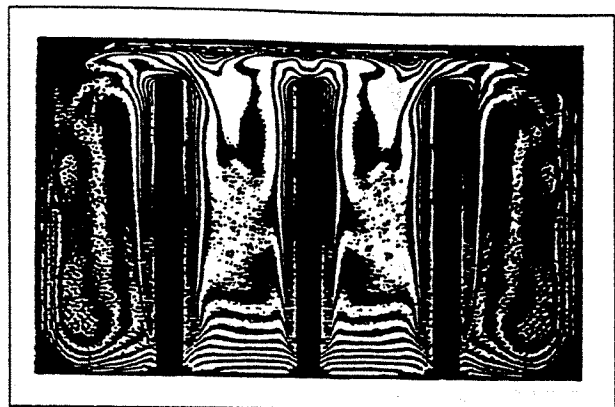


Fig. 4-2 Hologram in a 3-PCB's array  
 $Ra=1.55 \cdot 10^5$ ,  $t=t_0+0.5$  s,  
 $T_w=10^\circ\text{C}$ ,  $T_p=90^\circ\text{C}$ .

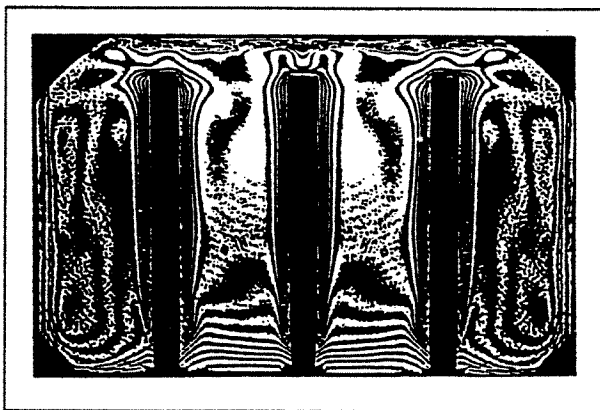


Fig. 4-3 Hologram in a 3-PCB's array  
 $Ra=1.55 \cdot 10^5$ ,  $t=t_0+1.0$  s,  
 $T_w=10^\circ\text{C}$ ,  $T_p=90^\circ\text{C}$ .

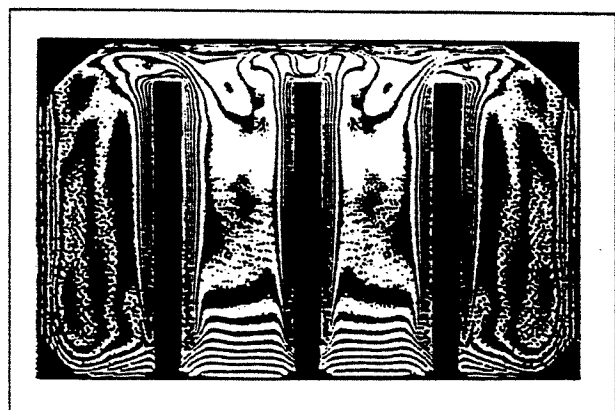


Fig. 4-4 Hologram in a 3-PCB's array  
 $Ra=1.55 \cdot 10^5$ ,  $t=t_0+1.5$  s,  
 $T_w=10^\circ\text{C}$ ,  $T_p=90^\circ\text{C}$ .

Fig. 4 Unsteady boundary layer on the top wall

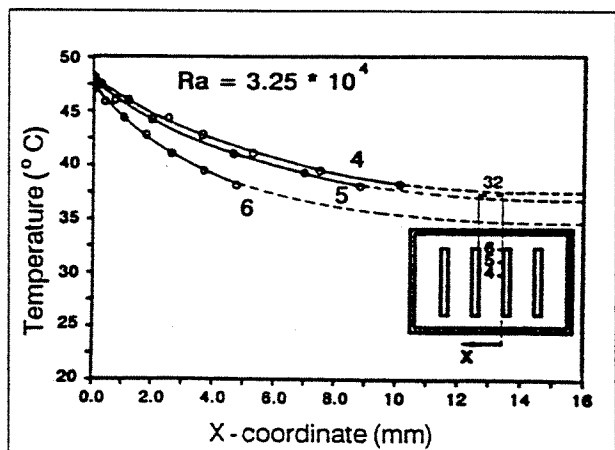
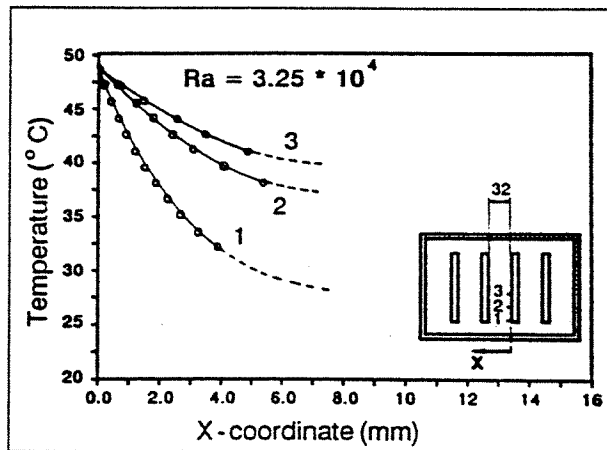


Fig. 5 Temperature profile in a channel of a 4-PCB's array

ations of heat transfer coefficients resulted from the thermal instability can be clearly seen.



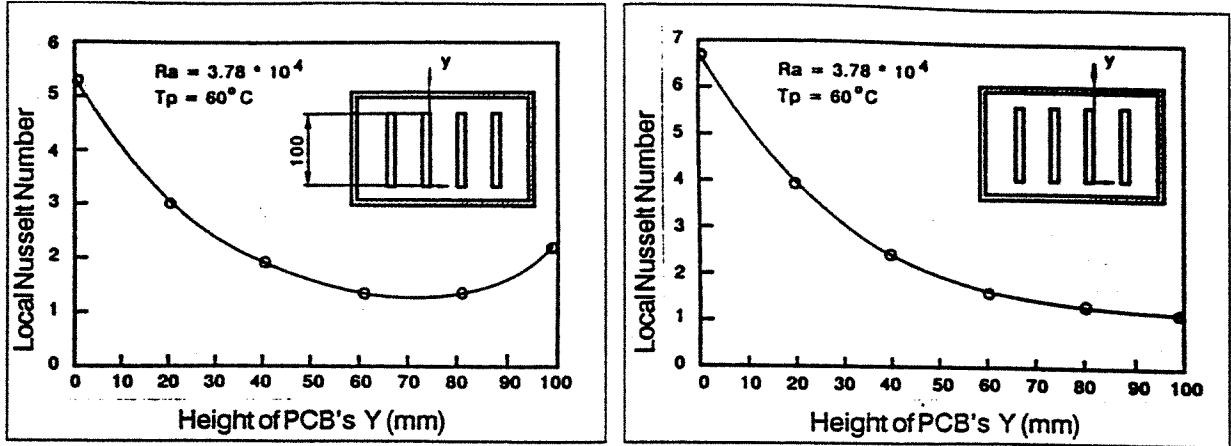


Fig. 6 Local Nu in two channels of a 4-PCB's array

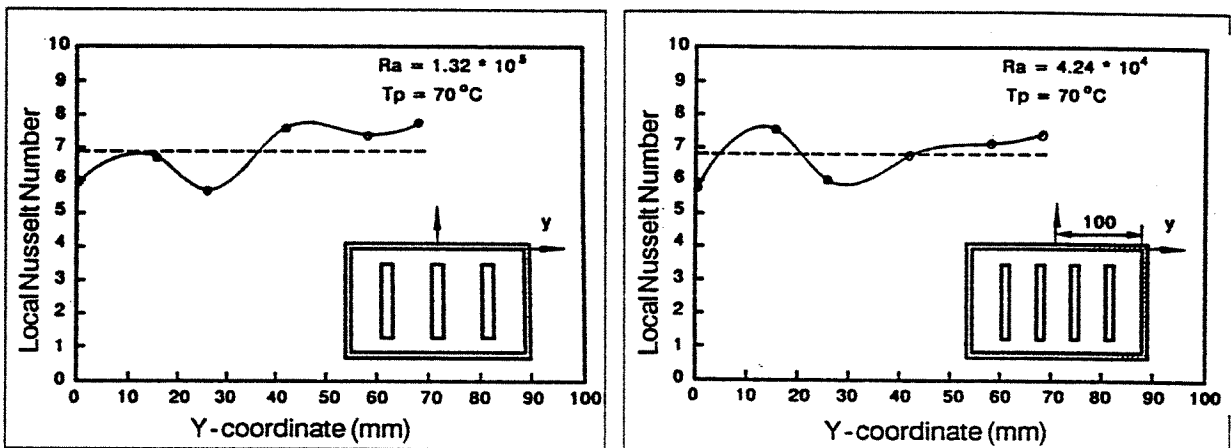


Fig. 7 Local Nu on the top wall of the casing

From Fig. 3-1 it can be observed that the waveform of the Nu-Y curve corresponds to the corrugated form of the thermal boundary layer on the top wall of the casing. The wave trough of the Nu-Y curve is in accordance with the wave trough of the thermal boundary layer, where the air in the vortex flow leaves the top wall. The wave crest of the Nu-Y curve is in accordance with the wave crest of the thermal boundary layer, where the air in vortex flow goes to the top wall. The similar phenomena were also found in ref. [13] where the phenomena of thermal instability produced by inner heat source in a hollow casing were investigated in detail. The wavelength of the corrugated-form boundary layer is dependent mainly on various geometric parameters. This relationship is demonstrated in Fig. 8.

For the thermal design of electronic equipments the relation between total heat load and temperature difference is more important. Determining the total heat load according to the given temperature rise and/or finding the maximum temperature rise on the basis of the given total heat load is one of fundamental tasks of thermal designers. From the experimental results correlation between averaged Nusselt number on all PCB's and

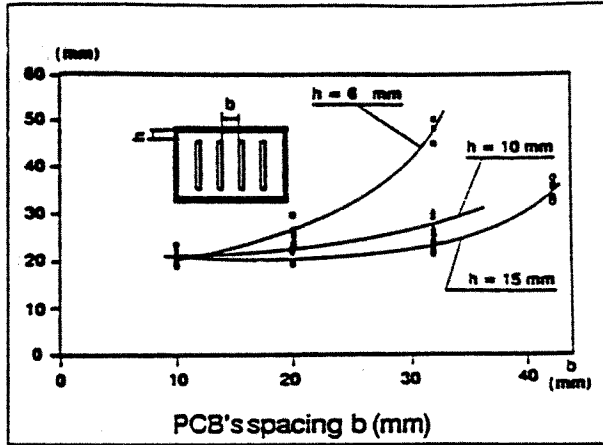


Fig. 8 The relation  $\lambda = f(b, h)$

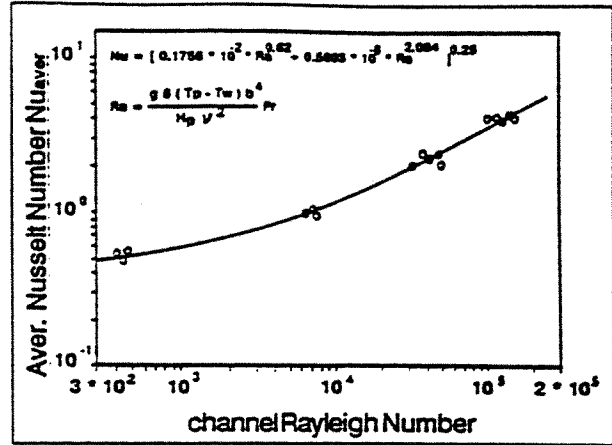


Fig. 9 The relation  $Nu=f(Ra)$

Rayleigh-number is as follows:

$$Nu_{aver} = \frac{1}{2N} \sum \overline{Nu} = [0.1756 * 10^{-2} * Ra^{0.62} + 0.5603 * 10^{-8} * Ra^{2.084}]^{0.25} \quad (5)$$

where  $Nu_{aver}$  is the averaged Nusselt-Number on each surface of each plate, and  $Ra$  the channel Rayleigh Number. The correlation is shown in Fig. 9.

## 2. Air circulation in the casing

Air circulation is an important factor affecting the cooling of the PCB's array in the casing. As the air in the PCB's array is warmed up by the dissipation heat of chips on the PCB's the warm air with lower density in the PCB's array goes up driven by buoyance force. Because of the existence of the top wall air flow has to take a turn to two side walls of the casing. When the side walls of the casing are cold the air flow falls down in the two side channels and goes again into the PCB's array after a turn on the bottom wall. As a whole, the overall natural convection flow can be divided into several circulation layers. When the situation is symmetrical the natural convective air flow produced in the central channel circulates in the most external layer and air stream from the channels next to the central one flows around the interior layers in sequence. Fig. 10 is a schematic drawing of this flow. This air circulation can be analysed with a simplified model which applies an integral approximation to turn the complex problem into a simple equivalent network. This network is shown in Fig.11.

In the network  $R_{ij}$ ,  $R_{ji}$  and  $R_i$  are flow resistances produced by wall friction and  $E_i$  are potentials produced by temperature difference between the PCB's array and the cold wall. The mean velocity in each channel plays here a role of current. When a temperature

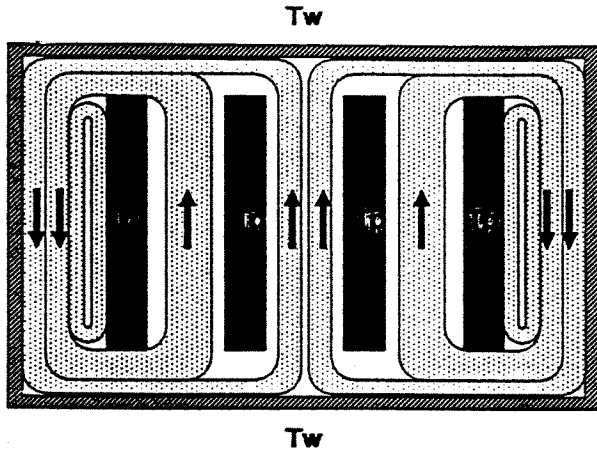


Fig. 10 Air circulation in the casing

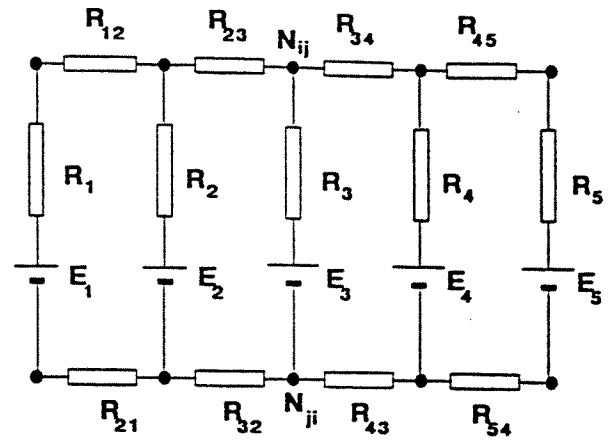


Fig. 11 Equivalent network of circulation

and a velocity profile are supposed the mean velocity can be found by using integral method and solving a group of nonlinear equations. Although there are many results on natural convection and heat transfer in PCB's array without the casing, it can be seen from Fig. 11 that the situations in PCB's array with or without a casing are quite different (When without a casing the knots  $N_{ij}$  and  $N_{ji}$  are directly grounded). The mean velocity distributions in a 8-PCB's array by two situations are shown in Fig. 12 and Fig. 13.

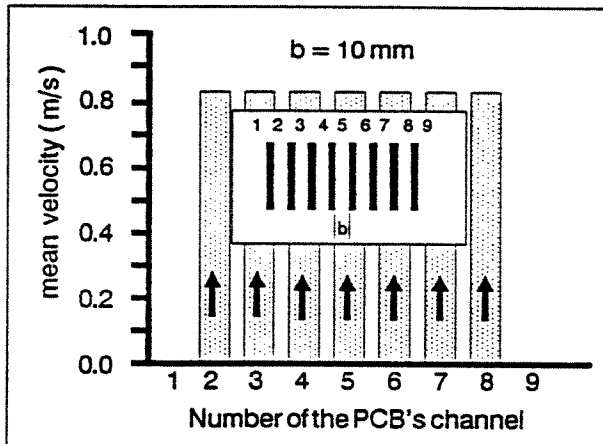


Fig. 12 mean velocity without a casing

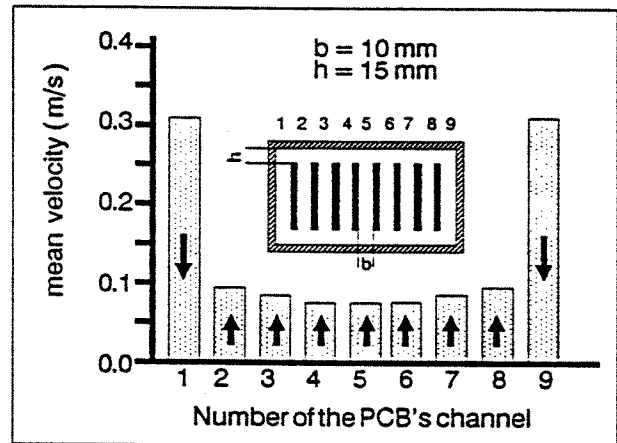


Fig. 13 mean velocity with a casing

From Fig. 12 and Fig. 13 it can be seen that the mean velocity in a PCB's array with a casing can be only about 1/10 the one in a same PCB's array but without a casing under the same temperature difference. When without a casing, the air flow at the entrance of a PCB's channel has the same temperature and depends only on the geometric parameters and temperature difference of this channel. Therefore the mean velocity is the same for each channel. By contrast, the air flow at the entrance of a PCB's channel with a casing has different temperature and is under the influence of other channels. The air flow in central channel has a longest path to circulate and therefore is smallest in quantity. Only

if the casing provides the PCB's array the sufficient down-flow channels the influence of the casing can be omitted.

### Conclusions

The holographic interferometry was used to investigate the flow and temperature field in the PCB's array with a casing and turned out to be a very good method to study the phenomena of natural convection in electronic equipments. Experimental results reveal that an unstable boundary layer is formed on the top wall of the casing because of the thermally unstable stratification of air in gravitational field. The thermal instability has good effect on the augmentation of heat transfer on the inner PCB's and also brings about the unfavourable influence of the fluctuations. Because of the existence of the casing the air circulation is greatly reduced. Temperature distribution, mean velocity and Nu relations are given. The empirical correlations are presented in the paper.

### Acknowledgement

The first author wishes to acknowledge the support of DAAD of F.R.G. and Lehrstuhl A für Thermodynamik, TU München.

### Nomenclature

Symbol	Quantity	Dimension
$a_i$	coefficients	[-]
b	PCB's spacing	[m]
$c_p$	specific heat capacity	[J/(K · kg)]
g	gravitational acceleration	[m/s <sup>2</sup> ]
h	distance between PCB's and the top wall	[m]
h	heat transfer coefficient	[W/K · m <sup>2</sup> ]
$H_p$	height of PCB's	[m]
H	height of casing	[m]
k	thermal conductivity	[W/K · m]
$L_x$	width of casing in x-direction	[m]
$L_z$	length of casing in z-direction	[m]

$q$	heat flux	$[W/m^2]$
$T_w$	casing wall temperature	$[K]$
$T_p$	PCB's temperature	$[K]$
$T_\infty$	surrounding temperature	$[K]$
$\bar{u}$	mean velocity in PCB's channels	$[m/s]$
$\alpha$	thermal diffusivity	$[m^2/s]$
$\beta$	expansion coefficient	$[1/K]$
$\nu$	kinematic viscosity	$[m^2/s]$
$x, y, z$	Cartesian coordinates	$[m]$
$Gr_n = \frac{\beta g \Delta T H_p^3}{\nu^2}$	Grashof number	$[-]$
$Nu = \frac{hb}{k}$	Nusselt number	$[-]$
$Pr = \frac{\nu}{\alpha}$	Prandtl number	$[-]$
$Ra = \frac{\beta g \Delta T b^3}{\nu \alpha} \frac{b}{H_p}$	channel Rayleigh number	$[-]$
$Ra_n = \frac{\beta g \Delta T H_p^3}{\nu \alpha}$	Rayleigh number	$[-]$

### References

1. W. Nakayama and A. E. Bergles, "Cooling Electronic Equipment: Past, Present, and Future", in Proc. of 20th International Symposium on Heat transfer in Electronic and Microelectronic Equipment, Aug. 29-Sept. 2, Dubrovnic, (1988).
2. A. Bar-cohen and W. M. Rohsenow, "Thermally Optimum Spacing of Natural Convection Cooled Parallel Plates", Transactions of the ASME, Vol. 106, pp. 116-123, (1984).
3. Johnson C.E., "Evaluation of Correlations for Natural Convection Cooling of Electronic Equipment", Heat transfer Engineering, Vol. 7, nos.1-2, (1986).
4. M. Ishizuka, Y. Miyazaki and T. Sasaki, "On the Cooling of Natural-air-cooled Electronic Equipment Casing", Bulletin of JSME, Vol. 29, No. 247, January (1986).
5. G. Guglielmini, G. Milano and M. Misale, "Some Factors Influencing the Optimum Free Air Cooling of Electronic Cabinets", in Proc. of 20th International

- Symposium on Heat transfer in Electronic and Microelectronic Equipment, Aug. 29-Sept. 2, Dubrovnic, (1988).
6. G. Guglielmini, G. Milano and M. Misale, "Free convection air cooling of ventilated electronic enclosures", in Proc. of second UK national conference on Heat transfer, Vol. 1, Sep. 14 - 16, U.K. (1988).
  7. G. Guglielmini, G. Milano and M. Misale, "Electronic cooling by natural convection in partially confined enclosures", Heat and Technology, Vol. 3, No. 3/4, (1985).
  8. M. Cadre, A. Viault, V. Pimont and A. Bourg, "Modeling of PCB's in Enclosure", in Proc. of 20th International Symposium on Heat transfer in Electronic and Microelectronic Equipment, Aug. 29-Sept. 2, Dubrovnic, (1988).
  9. W. M. Menschikow, B. S. Elkin, "Berechnungsmethode Stationärer Temperaturfelder in Elektronischen Geräten mit Freier Konvektion", Mitteilungen der Akademie der Wissenschaft der Armenischen SSR, XXXVI, No. 3, (1983).
  10. F. Mayinger, W. Panknin, "Holography in Heat and Mass transfer", in Proc. of 5th International Heat transfer Conference, VI, Tokio, (1974).
  11. Vest C.M., "Holographic Interferometry", John Wiley & Sons, New York, (1979).
  12. Becker H., U. Grigull, "Interferometrie transparenter Phasenobject, insbesondere bei hohen Interferenzstreifendichten, dargestellt an einem Beispiel aus der Wärmeübertragung", Wärme – und Stoffübertragung, pp. 233-244, 10 (1977).
  13. M. Jahn, "Holographische untersuchung der freien Konvektion in einer Kernschmelze", Dr.-Ing. thesis, T.U. Hannover, Hannover, F.R.G. (1975).